lengths on the same wafer stored in vacuum, whereas such behavior is readily understandable using the quantum-confinement model. More work is needed to help understand the mechanism of the PL emission.

Experimental

The irradiation of p-type silicon with 2 MeV He was carried out using a single-ended accelerator. The desired pattern was fed into the IONSCAN software which then controlled the beam scanning. The dose at each region was controlled by the amount of time the beam dwelled at that region. After irradiation, the samples were cleaned with diluted HF (< 10 %) and electrical contact was made to the backside of the samples using In–Ga eutectic paint and copper wire. A thick layer of epoxy was applied to protect the electrical contact during etching. Subsequently, the samples were electrochemically etched in a solution of HF/H_2O/ethanol (1:1:2) at constant current density for 5 min. The current densities used varied from 5–100 mA cm^{-2}. The etched samples were then washed in a mixture of 1:1 ethanol and water solution and transferred immediately to a vacuum chamber. All characterizations using micro-PL spectroscopy were taken in vacuum at room temperature using a 405 nm diode laser. The laser light was focused onto the sample through a ME600 Nikon microscope with a 100x objective. The PL signals were detected using a charge-coupled device (CCD) Ocean Optics Spectrometer by means of an optical fiber. Most of the laser light was cut off from the PL signal with a 495 nm long-pass filter. All spectra have been corrected for system response. For PL imaging, the samples were excited with a UV lamp through a 400 nm filter and captured with a CCD camera.

Received: June 3, 2005
Final version: September 24, 2005
Published online: November 21, 2005

[1] Z. H. Lu, D. J. Lockwood, J.-M. Baribeau, *Nature* **1995**, *378*, 258.
[2] L. Pavesi, L. Dal Negro, C. Mazzoleni, G. Franzo, F. Priolo, *Nature* **2000**, *408*, 440.
[3] H. Rong, R. Jones, A. Liu, O. Cohen, D. Hak, A. Fang, M. Paniccia, *Nature* **2005**, *433*, 725.
[4] L. T. Canham, *Nature* **2000**, *408*, 411.
[5] V. Lehmann, in *Electrochemistry of Silicon*, Wiley-VCH, Weinheim, Germany **2002**.
[6] L. T. Canham, *Appl. Phys. Lett.* **1990**, *57*, 1046.
[7] A. G. Cullis, L. T. Canham, *Nature* **1991**, *353*, 335.
[8] M. J. Sailor, E. J. Lee, *Adv. Mater.* **1997**, *9*, 783.
[9] S. Ossicini, L. Pavesi, F. Priolo, in *Light Emitting Silicon for Microphotonics*, Vol. 194, Springer-Verlag, Berlin, Germany **2003**, pp. 75–122.
[10] K. D. Hirschman, L. Tsybeskov, S. P. Duttagupta, P. M. Fauchet, *Nature* **1996**, *384*, 338.
[11] A. Briner, R. B. Wehrspohn, U. M. Gösele, K. Busch, *Adv. Mater.* **2001**, *13*, 377.
[12] V. V. Doan, M. J. Sailor, *Science* **1992**, *256*, 1791.
[13] S. P. Duttagupta, C. Peng, P. M. Fauchet, S. K. Kurinec, T. N. Blanton, *J. Vac. Sci. Technol. B* **1995**, *13*, 1230.
[14] M. Rocchia, S. Borini, A. M. Rossi, L. Boarino, G. Amato, *Adv. Mater.* **2003**, *15*, 1465.
[15] D. J. Sirbuly, G. M. Lowman, B. Scott, G. D. Stucky, S. K. Buratto, *Adv. Mater.* **2003**, *15*, 149.
[16] X. M. Bao, H. Q. Yang, F. Yan, *J. Appl. Phys.* **1993**, *79*, 1320.
[17] S. Chattopadhyay, P. W. Bohn, *J. Appl. Phys.* **2004**, *96*, 6888.
[18] E. J. Teo, D. Mangaiyarkarasi, M. B. H. Breese, A. A. Bettiol, D. J. Blackwood, *Appl. Phys. Lett.* **2004**, *85*, 4370.
[19] L. Pavesi, G. Giebel, F. Ziglio, G. Mariotto, F. Priolo, S. U. Campisano, C. Spinella, *Appl. Phys. Lett.* **1994**, *65*, 2182.
[20] J. F. Ziegler, J. P. Biersack, U. Littmark, in *The Stopping and Range of Ions in Solids*, Pergamon Press, New York **1985**.
[21] M. B. H. Breese, D. N. Jamieson, P. J. C. King, in *Materials Analysis using a Nuclear Microprobe*, Wiley, New York **1996**.
[22] J. A. van Kan, A. A. Bettiol, F. Watt, *Appl. Phys. Lett.* **2003**, *83*, 1629.
[23] L. T. Canham, A. G. Cullis, C. Pickering, O. D. Dosserm, T. I. Cox, T. P. Lynch, *Nature* **1994**, *368*, 133.
[24] B. G. Svensson, B. Mohadjeri, A. Hallen, J. H. Svensson, J. W. Corbett, *Phys. Rev. B* **1991**, *43*, 2292.
[25] B. G. Svensson, C. Jagadish, A. Hallen, J. Lalita, *Nucl. Instrum. Methods Phys. Res. Sect. B* **1995**, *106*, 183.
[26] A. Hallen, N. Keskitalo, F. Masszi, V. Nagi, *J. Appl. Phys.* **1996**, *79*, 3906.
[27] M. Yamaguchi, S. J. Taylor, Yang, S. Matsuda, O. Kawasaki, T. Hisamatsu, *J. Appl. Phys.* **1996**, *80*, 4916.
[28] P. Schmuki, L. E. Erickson, D. J. Lockwood, *Phys. Rev. Lett.* **1998**, *80*, 4060.
[29] Z. Gaburro, H. You, D. Babic, *J. Appl. Phys.* **1998**, *84*, 6345.
[30] M. V. Wolkin, J. Jorne, P. M. Fauchet, G. Allan, C. Delerue, *Phys. Rev. Lett.* **1999**, *82*, 197.
[31] L. Tsybeskov, J. V. Vandyshev, P. M. Fauchet, *Phys. Rev. B* **1994**, *49*, 7821.
[32] K. Y. Suh., Y. S. Kim, S. Y. Park, H. H. Lee, *J. Electrochem. Soc.* **2001**, *148*, C439.

DOI: 10.1002/adma.200501455

Self-Assembly Combined with Photopolymerization for the Fabrication of Fluorescence "Turn-On" Vesicle Sensors with Reversible "On–Off" Switching Properties**

By *Guangyu Ma*, *Astrid M. Müller*, *Christopher J. Bardeen*, and *Quan Cheng**

There is considerable interest in the development of self-amplifying polymeric materials that render direct fluorescence measurements of analytes by means of detecting changes of fluorescence intensity, wavelength, or lifetime.[1–3] Swager and co-workers have examined a series of conjugated polymers as the sensing material for a variety of molecular targets.[2,4–6] In these "smart" materials, the excited states (excitons) propagating along the conjugated backbone are quenched on encounter-

[*] Prof. Q. Cheng, G. Ma, Dr. A. M. Müller, Prof. C. J. Bardeen
Department of Chemistry, University of California
Riverside, CA 92521 (USA)
E-mail: quan.cheng@ucr.edu

[**] Q. C. acknowledges the support of the UC Riverside and the Eli Lilly analytical chemistry grant. C. J. B. acknowledges the support from NSF grant CHE-0517095. Supporting Information, including details of experimental procedure and characterization, is available online from Wiley InterScience or from the author.

ADVANCED MATERIALS

ing an energy trap at an occupied receptor site, leading to diminished fluorescence.[7] Leclerc and co-workers described a wavelength-shifting fluorescence measurement of DNA with cationic polythiophenes that allows for identification of a few hundred genome copies of a virus.[8,9] A highly desirable and more-sensitive approach is the development of fluorescence "turn-on" sensors in which the measured signal increases with target molecule concentration.[10–14] Several polymer-based systems have been developed for sensing that employ a quenching-recovery strategy, including the water-soluble poly(2,5-methoxypropyloxy sulfonate phenylenevinylene) (MPS-PPV) with biotinylated methylviologen, but interpretation of results is still debated.[15,16] Although elegant in design and highly effective for sensing, these sensing materials often involve complex organic synthesis.

We report here a novel and much more simplified approach for the fabrication of a self-amplifying fluorescence sensor by using self-assembly and photoinduced polymerization. The sensor is made by a vesicular assembly of lipids that consists of a conjugated polydiacetylene (PDA) moiety and a bleach-resistant, hydrophobic fluorescent dye. Polydiacetylenes have been well studied for their chromatic-transition properties and have been successfully employed for the development of colorimetric biosensors[17,18] for cholera toxin,[19] influenza virus,[20,21] *E. coli*,[22] epitopes,[23] and lipopolysaccharides.[24] The chromatic transition displayed in the colorimetric sensor is characterized by the distinct blue-to-red color change. The corresponding absorbance spectra exhibit a significant peak shift from 630 to 540 nm (Fig. 1). The PDA vesicles investigated in the present work for fluorescence sensing were prepared by mixing the two lipid components, Gly-PCDA and BODIPY dye BO558 (structures shown in Fig. 1), in the molar ratio of 100:0.5. Glycine derivatization of 10,12-pentacosadiynoic acid (PCDA) increases the size of the lipid headgroup and thus improves the vesicle formation, as compared to non-modified PCDA.[25] The excitation and emission spectra of BO558 are also shown in Figure 1. BODIPY is very photostable, making it suitable for this work since the polymerization of the diacetylene vesicles was achieved by using UV irradiation at 254 nm. After photopolymerization, the solution exhibits a blue-purple mixed color of the blue PDA and the pink BO558. Further characterization was carried out by dynamic light scattering (DLS) to measure the size change of the vesicles. Compared to vesicles made with phosphatidylcholine (PC) or PCDA, Gly-PCDA vesicles had a much larger average size, 350 ± 12 nm, probably due to the bulky headgroup of Gly-PCDA. After UV irradiation, these vesicles exhibited an approximately 60 nm reduction in diameter. The formation of covalent bonds between lipids apparently pulls the lipid molecules closer to each other.

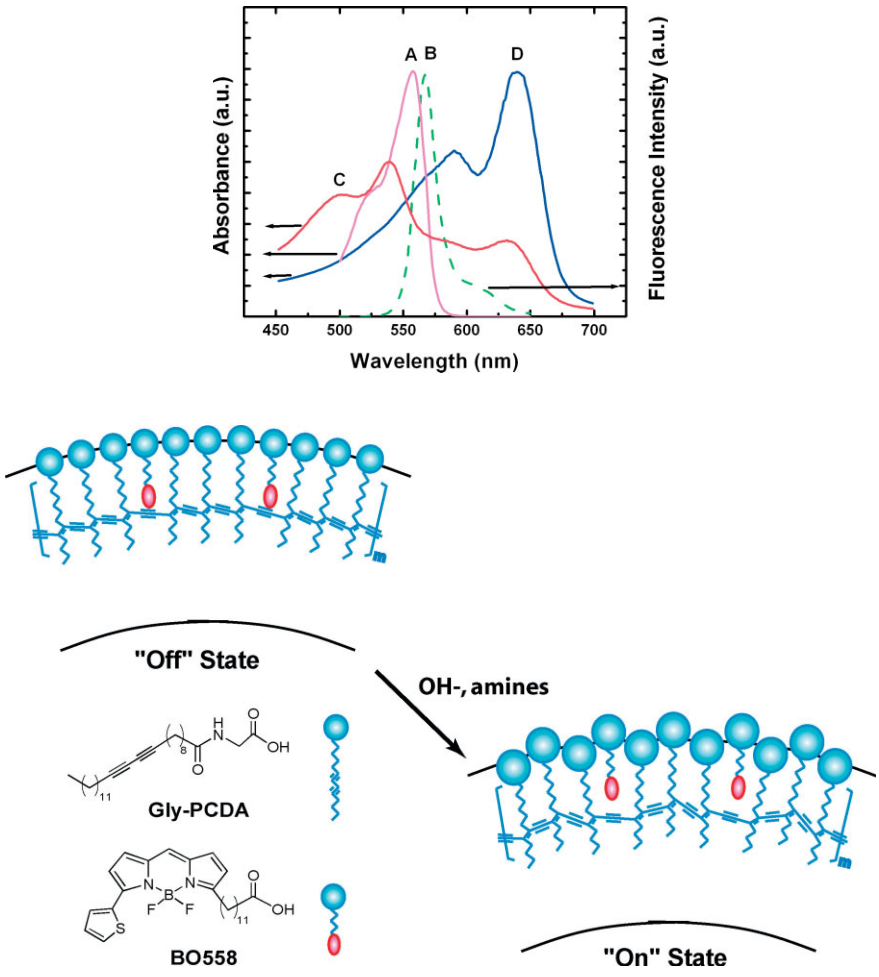

Figure 1. Top: Absorption and emission spectra of PDA and BODIPY dye BO558. Curves A, C, and D are absorption spectra of BO558, red-form PDA, and blue-form PDA, respectively; B is the emission spectrum of BO558. Bottom: Structure of lipid constituents used for fabrication of the vesicle sensor and a schematic illustration of the fluorescence "turn-on" mechanism. Only one leaflet of the vesicle membrane is shown for better demonstration of the dye position. PCDA: 10,12-pentacosadiynoic acid.

Before applying the sensor to target analytes, the "turn-on" properties of the vesicle sensor were tested in aqueous solution by changing the pH by means of adding various amounts of acid or base, and characterized by steady-state fluorescence spectroscopy (Fig. 2). Obviously, photopolymerization of the diacetylene lipids leads to a substantial quenching of BO558 dye in the vesicles. The fluorescence intensity decreased by more than 60 % (curve 2) as compared to that before irradiation (curve 1). When the vesicle solution was treated with

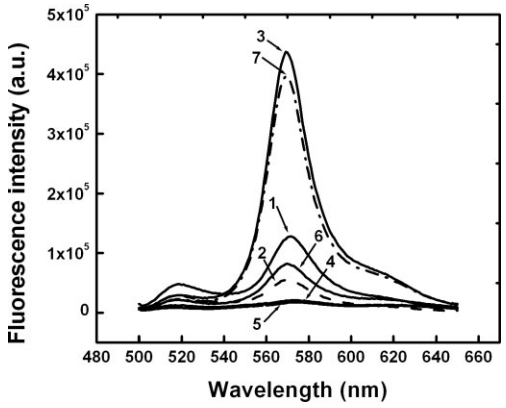

Figure 2. Fluorescence spectra of the Gly-PDA/BO558 vesicle system in response to acid/base addition under various solution conditions. Curves 3–7 show subsequent addition of either acid or base into the testing solution. 1) Before UV irradiation; 2) after 1 min UV irradiation; 3) addition of 20 μL 0.1 M NaOH; 4) addition of 20 μL 0.1 M HCl; 5) addition of 20 μL 0.1 M HCl; 6) addition of 20 μL 0.1 M NaOH; 7) addition of 20 μL 0.1 M NaOH.

20 μL of 0.1 M NaOH, however, the fluorescence intensity showed an enormous increase, far exceeding the original intensity before UV irradiation. Importantly, the degree of increase in intensity is affected by the amount of the basic solution added and its concentration. More interestingly, subsequent addition of 20 μL 0.1 M HCl solution "quenched" the fluorescence signal, reducing the emission intensity to below curve 1 (curve 4 in Fig. 2). Further quenching was observed when an additional 20 μL of 0.1 M HCl solution was added, leading to more reduction of the fluorescence intensity (curve 5). It is important to point out that this process is totally reversible. When more NaOH solution was added again to the vesicle solution, the fluorescence emission could be recovered, demonstrating a unique "on–off" switching behavior. The change of vesicle size during the switching process was monitored by DLS. When treated with 0.1 M NaOH, the PDA vesicles showed a slight increase of about 20 nm in size, most likely due to Coulombic repulsion of the deprotonated carboxylic headgroups in a basic solution.

To understand the effect of UV irradiation and addition of basic solution on the properties of BO558 dye, comparison experiments were carefully performed on BO558-containing vesicles prepared from the saturated lipid L-α-phosphatidylglycerol (PG). Unlike the diacetylene vesicles, a strong fluorescence signal was observed before UV irradiation, and the intensity was similar to that of the free BO558 of the same amount dissolved in organic solvent. Irradiation at 254 nm for 1 min led to less than a 10 % decrease of the fluorescence intensity. Addition of 0.1 M NaOH resulted in a slight decrease of the intensity rather than an increase. Therefore, the gain in fluorescence intensity that was observed in the PDA vesicles is not a direct result of the base acting on the dye. In other words, BO558 itself is insensitive to either UV or sodium hydroxide. The quenching effect must be due to some interaction of the dye with the PDA vesicles.

The emission spectrum of BO558 has a good overlap with the absorption spectra of both blue and red PDA, as depicted in Figure 1. Excitation-energy migration between polymer and dye molecules has been reported.[26] In our case, the dispersive transport of emission energy from the excited fluorophore (BO558) to the conjugated polymer backbone is energetically allowed. In fact, BO558 incorporated into the diacetylene vesicles had already demonstrated a significant quenching even before polymerization. The intensity decreases by about 90 %, as compared to free dye molecules dissolved in methanol. In contrast, vesicles prepared from saturated PG lipids exhibited a fluorescence intensity similar to that of free BO558 molecules in organic solvent. After polymerization, the quenching efficiency in PDA vesicles increases to above 95 %. The BO558 dye is confined within the vesicle membrane and leakage is insignificant. This was confirmed by filtration of the BO558 doped-vesicle solution with a 10 000 g mol^{-1} molecular weight cut-off membrane, where less than 2 % of the original fluorescence intensity was observed in the filtrate.

The mechanism of quenching is important to understand in order to optimize sensor performance. One can envision two limiting cases for the fluorescence quenching in these vesicles: dynamic versus static.[27] In the first case, the BO558 dye is randomly distributed within the vesicle, and as the pH increases, the average distance between BO558 and the PDA segments increases, leading to reduced quenching. This mechanism relies on a quenching process, for example Förster energy transfer, where the quenching probability depends strongly on distance ($1/R^6$, where R is the intermolecular distance). Such dynamic quenching between the diffusing dye and PDA segments can be contrasted with a static mechanism, where some fraction of dye is associated with a specific site in the PDA vesicles which completely quenches its fluorescence. PDA vesicles of this type have previously been hypothesized to undergo conformational changes in response to pH,[25] and these different conformations could provide such quenching sites.

In order to distinguish between these two mechanisms, a more detailed analysis of the spectroscopy is required. The fluorescence spectrum of the vesicle solution reflects the presence of two emitting species: the weak, red PDA fluorescence with peaks at 520 and 570 nm, and the more intense BO558 fluorescence with a peak at 575 nm. The overlap of these emissions complicates the analysis of the spectral data, so we have used time-resolved fluorescence spectroscopy to help establish the mechanism of fluorescence quenching. The normalized fluorescence decays at three different pH values (pH 7.0, 8.9, 10.0) are shown in Figure 3a. At all pH values, there is a fast, early time decay on the order of 100 ps, which is due to the fluorescence decay of the red PDA. This is followed by a much slower decay, whose spectral shape is identical to that of BO558. A comparison of the early and late fluorescence spectra for pH 10.0 and pH 7.0 is depicted in Figures 3b,c. Note that the contrast between pH 7.0 and pH 10.0 is even greater in the 1–17 ns window than it is in the steady-

ADVANCED MATERIALS

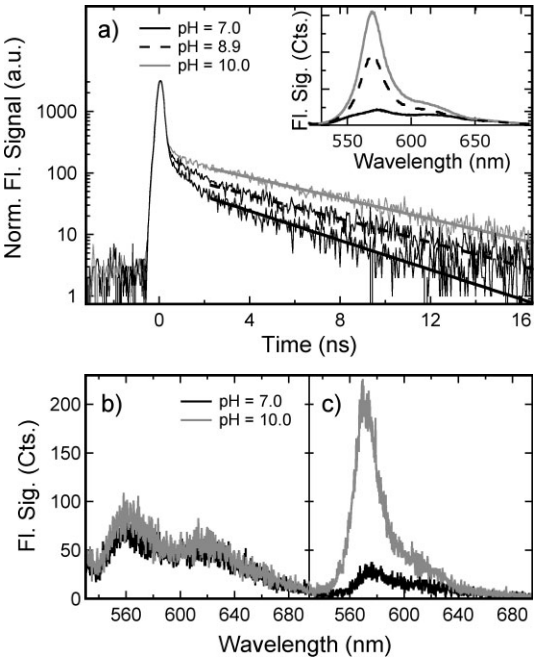

Figure 3. a) Time-resolved fluorescence decays of the Gly-PDA/BO558 vesicles at pH 10.0 (gray line), pH 8.9 (dashed) and pH 7.0 (solid black). The straight lines are single-exponential fits to the long-lived component of the decays as described in the text. The corresponding steady-state fluorescence spectra are shown in the inset. b) The spectrum of the Gly-PDA/BO558 vesicle fluorescence in the time window –3.3–0.3 ns for pH 10.0 (grey) and pH 7.0 (black). For both pH values, the short-time fluorescence is dominated by the red PDA contribution. c) The spectrum of the Gly-PDA/BO558 vesicle fluorescence in the time window 0.7–16.8 ns for pH 10.0 (grey) and pH 7.0 (black). At the high pH, the long-lived spectrum is identical to that of BO558, while at the lower pH only residual red PDA emission is observed, which is at least eight times less intense.

state data shown in Figure 2. This suggests that a time-gated detection, which effectively removes the PDA contribution to the fluorescence, could achieve even higher sensitivity to changes in pH than the steady-state measurement, although at the cost of increased experimental effort. As the pH is lowered, the amplitude of the long-lived decay decreases, while the short-lived component remains unaffected. Thus, the decrease in the steady state fluorescence is almost entirely due to quenching of the BO558 fluorescence at lower pH.

One potential mechanism for the observed quenching is Förster energy transfer from the excited BO558 molecules floating in the vesicles to the PDA-lipid framework. As mentioned above, the strong overlap of BO558 emission with the absorption spectrum of the blue PDA component of the vesicles suggests that facile energy transfer is possible. Assuming that BO558 molecules remain associated with the vesicles over the pH range used here, the increase in fluorescence intensity would be due to increased intermolecular distances, possibly the result of vesicle swelling in more basic environments. If this were the case, we would expect to see a continuous change in fluorescence lifetime as the BO558 fluorescence decreases. From Figure 3, this is clearly not the case. For example, the decay time of the long-lived emission changes from 6.2 ns at pH 10.0 to 5.3 ns at pH 8.9, a decrease of only 15 %, while the amplitude of the BO558 steady-state fluorescence decreases by about 60 %. The fact that the fluorescence decay time hardly changes while the fluorescence intensity declines dramatically would appear to rule out a conventional dynamic quenching process, either due to Förster energy transfer or due to some other rate-driven process. As an additional check, we used light scattering and transmission electron microscopy (TEM) to characterize the size changes of vesicles as a function of pH. After treatment with NaOH solution, the size of the Gly-PDA vesicles increased by about 20 nm. In a basic environment, we hypothesize that the deprotonated carboxylic acid head groups repel each other and cause swelling of the vesicles. The increase in particle size at high pH would suggest an increase in intermolecular distance as well. But, this distance will be linearly proportional to the diameter, and the 6 % increase in average distance R would only correspond to a 32 % change in quenching rate, assuming a $1/R^6$ Förster mechanism. Again, this relatively small change is inconsistent with the much larger quenching observed in the steady-state spectra.

Since the data are inconsistent with a simple dynamic Förster mechanism for the quenching, we hypothesize that it is instead due to a static mechanism based on a pH-dependent association of BO558 with the PDA-vesicle framework. This static quenching process would not affect the lifetime, but the fluorescence would be either on or off depending on whether the BO558 molecule is bound or unbound. Both BO558 and the functionalized PCDA used to form the vesicles possess carboxylic acid groups, which will be completely deprotonated at pH 10.0. In this case, Coulombic repulsion should prevent association of the two molecules, in the same way that it leads to swelling of the vesicles. Rather than changing the average intermolecular distance, however, increasing the pH would shift the equilibrium from bound to unbound dye, leading to more fluorescence. Figure 1 provides a schematic illustration of the bound ("off") and unbound ("on") states. At high pH, the increased head group size can not be accommodated by the original packing. Since the polymer chain prevents free expansion, as would be the case in unpolymerizable vesicles, the carboxylate head group would take a staggered arrangement to minimize the impact.[25] Because the dye molecules are not covalently linked to the polymer backbone, they would most likely be pushed towards the vesicle periphery, generating an "unbound" state that shows high fluorescence. At low pH, the staggered packing is reversed, restoring the quenching properties. It is worth noting that lowering solution pH does not entirely restore the polymer-backbone conformation as the blue-to-red chromatic transition is irreversible under this condition. Nevertheless, the fluorescence "on–off" switching property can be obtained with the red form of PDA vesicles.

From this model, the lifetime of the unbound dye at all pH values would be expected to be similar to that of BO558 in the absence of PDA (5.5 ns in ethanol). This has been confirmed experimentally. Incorporation of non-polymerizable lipids such as PC or ganglioside GM1 into the vesicles lowers

the number of quenching sites and weakens the quenching effect (data not shown), as expected for a static binding mechanism. Whether this quenching is due to energy transfer or electron transfer is unknown at this time. The fact that the sensor can be cycled multiple times through high and low pH suggests that the quenching does not lead to an irreversible chemical reaction, as is sometimes the case in electron-transfer quenching. However, further studies are necessary to identify the molecular mechanism of the quenching. What we can say with certainty is that the combination of steady-state and time-resolved fluorescence measurements, along with characterization of the vesicles' morphology using TEM and light scattering, all suggest that the fluorescence is controlled by a pH-dependent association with the crosslinked PDA lipid.

In order to demonstrate the sensing function of the novel vesicular assemblies, different amounts of three organic amines (triethylamine, diisopropylamine, and benzylamine) were added to the BO558-doped Gly-PCDA vesicle solutions, and the steady-state fluorescence data were recorded. The results are shown in Figure 4. The measured fluorescence intensity depends linearly on the amine concentration in the range of 10 μM to 0.2 mM for all investigated amines. The detection sensitivity (slope) appears to be associated with

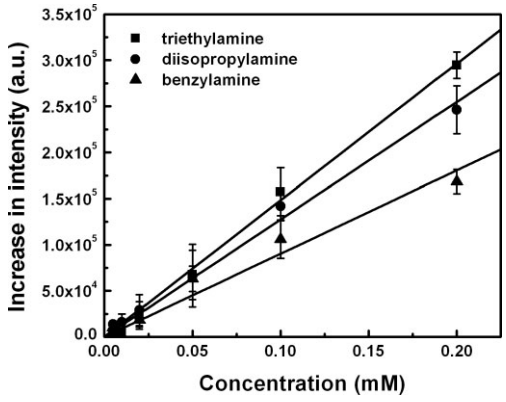

Figure 4. Calibration curves of the Gly-PDA/BO558 vesicle sensors for the detection of triethylamine, diisopropylamine, and benzylamine in the concentration range 5–200 μM.

the basicity of the amine compounds. The three amine compounds can be preliminarily differentiated by the different slopes of the calibration curves. Among the three compounds, triethylamine is the most basic ($pK_a = 10.80$) and diisopropylamine is similar ($pK_a = 10.76$), while the primary amine benzylamine is a considerably weaker base ($pK_a = 9.40$). Using the 3σ cutoff, the detection limit was determined to be 3.0 μM for triethylamine, 4.4 μM for diisopropylamine, and 5.7 μM for benzylamine. This test demonstrates that the vesicle sensor system is well suited for fluorescence detection with exceptional sensitivity for small molecular compounds.

In conclusion, we have developed a novel, self-amplifying, conjugated polymeric vesicle sensor with reversible "on–off" switching properties by employing a relatively simple photopolymerization process for fabrication. As first examples for "on–off" sensing operation, we have shown that the fluorescence intensity of BO558-doped PDA vesicles can be manipulated by experimental conditions such as solution pH or amount of added organic amine. The "on" state of the fluorescent molecules is a result of formation of an unbound state due to the staggered lipid arrangement induced by electrostatic repulsion at high pH. The rapid, reversible, and sharp response to external stimuli provides a new platform for sensing applications. As a consequence, the BO558-PDA system offers great potential for future use in bioanalyte sensing, since any process that alters the backbone/fluorophore association will lead to changes in fluorescence intensity. Future work will focus on optimization of the system to enhance the background fluorescence suppression by screening photoresistant dyes that have less absorption overlap with the PDA-conjugated backbone. We will also attempt the incorporation of bioselective units into the vesicles in order to detect biological targets using the self-amplification mechanism.

Experimental

Materials: 10,12-Pentacosadiynoic acid (PCDA) was purchased from GFS Chemicals (Powell, OH). The Gly-PCDA lipid was synthesized according to a published procedure [25] and verified by NMR and mass spectrometry. 4,4-Difluoro-5-(2-thienyl)-4-bora-3*a*,4*a*-diaza-*s*-inda-cene-3-dodecanoic acid (BODIPY 558/568C_{12}, abbreviated as BO558) was purchased from Molecular Probes (Eugene, OR). Vesicles were prepared by probe sonication. The detail of vesicle preparation and characterization is provided in the Supporting Information.

Steady-State Fluorescence Measurements: Fluorescence measurements were performed on a HORIBA FluoroLog spectrofluorometer using the excitation at 475 nm. For the pH-effect experiments, 20 μL of 0.1 M NaOH or 0.1 M HCl was added into a 600 μL vesicle solution. For organic amine tests, 50 μL of different amine solutions with concentration ranging from 100 μM to 2 mM was added into a 450 μL vesicle solution in a cuvette to make the total volume 500 μL.

Lifetime Fluorescence Measurements: Steady-state UV-vis absorption and fluorescence data of the samples with pH 7.0, 8.9, and 10.0 were recorded using a Cary 50 Bio UV-vis spectrometer and a Spex Fluorolog Tau-3 fluorescence spectrophotometer (excitation at 500 nm), respectively. The pH values of the samples were determined using a pH meter. Samples were prepared with a peak optical density of less than 0.2 in order to prevent self-absorption effects. Fluorescence lifetimes were measured upon exciting the samples with short pulses centered at 500 nm. The light pulses were generated by a 40 kHz regeneratively amplified Ti:sapphire laser system and a nonlinear optical parametric amplifier [28]. Samples were measured in 1 cm path length disposable plastic cuvettes, and the fluorescence emission was collected at 90° relative to the excitation. The excitation pulses exhibited linear polarization parallel to the detection axis, and the angle between the polarization of the collected fluorescence light and that of the excitation light was adjusted to 54.7° (magic angle) using a thin-film polarizer in order to eliminate an additional unwanted time-dependence signal due to molecular reorientation. The fluorescence light was directed into a monochromator attached to a picosecond streak camera (Hamamatsu C4334 Streakscope), which provided both time- and wavelength-resolved fluorescence data with resolutions of 15 ps and 2.5 nm, respectively.

Received: July 16, 2005
Final version: September 13, 2005
Published online: November 21, 2005

ADVANCED MATERIALS

[1] D. T. McQuade, A. E. Pullen, T. M. Swager, *Chem. Rev.* **2000**, *100*, 2537.
[2] T. H. Kim, T. M. Swager, *Angew. Chem. Int. Ed.* **2003**, *42*, 4803.
[3] S. L. Wiskur, H. Ait-Haddou, J. J. Lavigne, E. V. Anslyn, *Acc. Chem. Res.* **2001**, *34*, 963.
[4] J. S. Yang, T. M. Swager, *J. Am. Chem. Soc.* **1998**, *120*, 11 864.
[5] S. W. Zhang, T. M. Swager, *J. Am. Chem. Soc.* **2003**, *125*, 3420.
[6] T. Shioya, T. M. Swager, *Chem. Commun.* **2002**, 1364.
[7] K. Kuroda, T. M. Swager, *Macromol. Symp.* **2003**, *201*, 127.
[8] H. A. Ho, M. Boissinot, M. G. Bergeron, G. Corbeil, K. Dore, D. Boudreau, M. Leclerc, *Angew. Chem. Int. Ed.* **2002**, *41*, 1548.
[9] K. Dore, S. Dubus, H. A. Ho, I. Levesque, M. Brunette, G. Corbeil, M. Boissinot, G. Boivin, M. G. Bergeron, D. Boudreau, M. Leclerc, *J. Am. Chem. Soc.* **2004**, *126*, 4240.
[10] D. T. McQuade, A. H. Hegedus, T. M. Swager, *J. Am. Chem. Soc.* **2000**, *122*, 12 389.
[11] L. J. Fan, Y. Zhang, W. E. Jones, *Macromolecules* **2005**, *38*, 2844.
[12] S. Uchiyama, N. Kawai, A. P. de Silva, K. Iwai, *J. Am. Chem. Soc.* **2004**, *126*, 3032.
[13] H. Tong, L. X. Wang, X. B. Jing, F. S. Wang, *Macromolecules* **2003**, *36*, 2584.
[14] B. Liu, G. C. Bazan, *Chem. Mater.* **2004**, *16*, 4467.
[15] L. H. Chen, D. W. McBranch, H. L. Wang, R. Helgeson, F. Wudl, D. G. Whitten, *Proc. Natl. Acad. Sci. USA* **1999**, *96*, 12 287.
[16] S. J. Dwight, B. S. Gaylord, J. W. Hong, G. C. Bazan, *J. Am. Chem. Soc.* **2004**, *126*, 16 850.
[17] J. M. Kim, E. K. Ji, S. M. Woo, H. W. Lee, D. J. Ahn, *Adv. Mater.* **2003**, *15*, 1118.
[18] W. Spevak, J. O. Nagy, D. H. Charych, *Adv. Mater.* **1995**, *7*, 85.
[19] D. Charych, Q. Cheng, A. Reichert, G. Kuziemko, M. Stroh, J. O. Nagy, W. Spevak, R. C. Stevens, *Chem. Biol.* **1996**, *3*, 113.
[20] D. H. Charych, J. O. Nagy, W. Spevak, M. D. Bednarski, *Science* **1993**, *261*, 585.
[21] A. Reichert, J. O. Nagy, W. Spevak, D. Charych, *J. Am. Chem. Soc.* **1995**, *117*, 829.
[22] Z. F. Ma, J. R. Li, M. H. Liu, J. Cao, Z. Y. Zou, J. Tu, L. Jiang, *J. Am. Chem. Soc.* **1998**, *120*, 12 678.
[23] S. Kolusheva, R. Kafri, M. Katz, R. Jelinek, *J. Am. Chem. Soc.* **2001**, *123*, 417.
[24] M. Rangin, A. Basu, *J. Am. Chem. Soc.* **2004**, *126*, 5038.
[25] Q. Cheng, R. C. Stevens, *Langmuir* **1998**, *14*, 1974.
[26] K. Brunner, J. A. E. H. van Haare, B. M. W. Langeveld-Voss, H. F. M. Schoo, J. W. Hofstraat, A. van Dijken, *J. Phys. Chem. B* **2002**, *106*, 6834.
[27] J. R. Lakowicz, *Principles of Fluorescence Spectroscopy*, 2nd ed., Kluwer Academic, New York **1999**.
[28] T. Wilhelm, J. Piel, E. Riedle, *Opt. Lett.* **1997**, *22*, 1494.

DOI: 10.1002/adma.200501600

Controlled Synthesis of Abundantly Branched, Hierarchical Nanotrees by Electron Irradiation of Polymers**

By *Sung Oh Cho*,* *Eun Je Lee*, *Hyeok Moo Lee*, *Jin Gyu Kim*, and *Youn Joong Kim*

One-dimensional (1D) nanostructures such as nanowires, nanorods, nanobelts, and nanotubes, have attractive electronic, mechanical, and optical properties and can be applied in various nanodevices.[1–4] Thus, the synthesis of 1D nanostructures has become the focus of intensive research. Several routes to these nanostructures have been developed, including chemical vapor deposition,[3,4] a solution–liquid–solid method,[5] template-directed synthesis,[6] laser ablation,[7] and particle-beam-induced deposition.[8] Recently, multiply branched, three-dimensional (3D) hierarchical nanostructures, based on the 1D structures, have been fabricated.[9–13] Hierarchical nanostructures have large surface areas and allow for heterostructures; thus, they can be applied in photovoltaics and multifunctional nanoelectronics. In this report we present a novel synthesis route to yield 3D hierarchical, tree-like nanostructures with controlled morphologies, consisting of trunks and abundant branches. The proposed route is based on electron irradiation of inorganic polymers, and it does not require any catalysts, templates, or high-temperature processing environment. This route promises a straightforward means to fabricate complex hierarchical organic–inorganic nanostructures.

The polymeric precursors used in the experiments were silicon-based inorganic polymers, poly(dimethylsiloxane) (PDMS), and silicone compounds (see Experimental). The polymers were deposited on copper substrates and subsequently irradiated with an electron beam, which was generated from a thermionic electron gun.[14] Irradiation was carried out at ambient temperature in a vacuum chamber. The polymeric precursors were colorless; however, we observed that a black material coated the substrates after electron irradiation. Detailed morphologies of the electron-irradiated polymer specimens have been investigated by field-emission

[*] Prof. S. O. Cho, E. J. Lee, H. M. Lee
Department of Nuclear and Quantum Engineering
Korea Advanced Institute of Science and Technology
Daejon 305-701 (Korea)
E-mail: socho@kaist.ac.kr
J. G. Kim, Dr. Y. J. Kim
Electron Microscopy Team
Division of Nanomaterials and Environmental Sciences
Korea Basic Science Institute
Daejeon 305-333 (Korea)

[**] Supporting Information is available online from Wiley InterScience or from the author.